PHYSICAL REVIEW A **71**, 060310(R) (2005)

Efficient high-fidelity quantum computation using matter qubits and linear optics

Sean D. Barrett* and Pieter Kok†
Hewlett Packard Laboratories, Filton Road, Stoke Gifford, Bristol BS34 8QZ, United Kingdom
(Received 3 August 2004; revised manuscript received 3 February 2005; published 24 June 2005)

We propose a practical, scalable, and efficient scheme for quantum computation using spatially separated matter qubits and single-photon interference effects. The qubit systems can be nitrogen-vacancy centers in diamond, Pauli-blockade quantum dots with an excess electron, or trapped ions with optical transitions, which are each placed in a cavity and subsequently entangled using a double-heralded single-photon detection scheme. The fidelity of the resulting entanglement is extremely robust against the most important errors such as detector loss, spontaneous emission, and mismatch of cavity parameters. We demonstrate how this entangling operation can be used to efficiently generate *cluster states* of many qubits, which, together with single-qubit operations and readout, can be used to implement universal quantum computation. Existing experimental parameters indicate that high-fidelity clusters can be generated with a moderate constant overhead.

DOI: 10.1103/PhysRevA.71.060310 PACS number(s): 03.67.Lx, 03.67.Pp, 32.80.−t, 78.70.−g

Quantum computation (QC) offers a potentially exponential computational speed-up over classical computers, and many physical implementations have been proposed. Particularly promising proposals are those in which unitary operations and readout in matter qubits are implemented via laser-driven optical transitions. Examples include the original ion-trap proposal [1], nitrogen-vacancy (NV) centers in diamond [2], and schemes utilizing the Pauli-blockade effect in quantum dots with a single excess electron [3,4]. Single-qubit operations and readout, using a combination of optical and radio-frequency (RF) control fields, have already been demonstrated in ion-trap and NV-diamond systems [2,5,6], while a number of promising techniques for optically addressing quantum dot spin qubits have been proposed [3,4]. In all these cases, the ratio of the single-qubit operation time to the intrinsic decoherence times suggests that very high-fidelity operations are possible.

However, there are substantial difficulties in *scaling* these implementations to the large numbers of qubits required for useful QC. Multiqubit gates are facilitated by a direct interaction between qubits. Thus adding a new qubit to a quantum register, together with the associated control fields, necessarily modifies the Hamiltonian of the system. This can mean that, as more qubits are added, logic gate implementations become progressively more complex, and new decoherence channels can be introduced. Furthermore, the need to optically address individual qubits can lead to seemingly contradictory system requirements: the qubits need to be sufficiently well separated to be resolved by the optical field, but must be close enough such that two-qubit logic can be implemented via the interqubit interaction.

Our proposed solution to these scaling challenges is to perform *distributed* quantum computing, in which the matter qubits are spatially separated, and there is no direct interaction between the qubits. Instead, entangling operations (EOs) between qubits are implemented via single-photon interference effects. Several schemes to entangle pairs of distant qubits in this way have been proposed [7]. Recently, it has been shown that unitary logic gates can be performed in this manner [8,9]. However, the latter schemes are either inherently nondeterministic [9] or are sensitive to photon loss or photodetector inefficiency [8] and it is not clear whether they can be used for scalable QC. Schemes using single-photon interference effects together with local *two-qubit* unitary operations have also been proposed [10,11].

In this paper, we propose a *fully scalable* scheme for distributed QC using individual matter qubits assuming only single-qubit operations. Our scheme is robust to photon loss and other sources of errors, and uses optical transitions of the qubit system, together with linear optics and photodetection to entangle pairs of spatially separated matter qubits in a nondeterministic manner. A key observation is that even such a nondeterministic EO is sufficient for scalable QC: our EO can be used to efficiently generate *cluster states* of many qubits, which, together with single-qubit operations and measurements, are capable of universal QC [12]. In the context of linear optics QC [13], it has recently been shown [14–16] that the cluster state model can be used to significantly reduce the resource overheads required for scalable QC.

We consider matter systems comprised of two long-lived, low-lying states $|\uparrow\rangle$ and $|\downarrow\rangle$, and one excited state $|e\rangle$, in an L configuration (see Fig. 1). The system is constructed in such a way that an optical π pulse will induce the transformation $|\downarrow\rangle \rightarrow |e\rangle$ and $|\uparrow\rangle \rightarrow |\uparrow\rangle$. The transition $|\uparrow\rangle \leftrightarrow |e\rangle$ is forbidden, e.g., by a selection rule. The states $|\uparrow\rangle$ and $|\downarrow\rangle$ represent the logical qubit states $|0\rangle$ and $|1\rangle$, respectively. We assume that high-fidelity single-qubit operations and measurements can be performed on these logical qubits. Physical systems that have a suitable level structure include NV centers in diamond [2], quantum dots with a single excess electron [3,4], and various trapped ion and atomic systems. Each such system is embedded in a separate optical cavity, such that only the $|\downarrow\rangle \leftrightarrow |e\rangle$ transition is coupled to the cavity mode. One end of each cavity is leaky, with the leakage rate of the ith cavity given by $2\kappa_i$. The light escaping from the cavities is mixed on a 50:50 beam splitter (BS), the output modes of

*Electronic address: sean.barrett@hp.com
†Electronic address: pieter.kok@hp.com

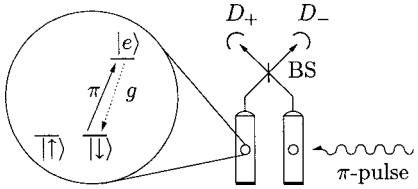

FIG. 1. In the circle: The qubit system $\{|\uparrow\rangle, |\downarrow\rangle\}$ with the excited state $|e\rangle$. The π pulse affects only the transition $|\downarrow\rangle \rightarrow |e\rangle$, and the emission of a photon into the cavity mode brings the excited state back to the qubit state $|\downarrow\rangle$. Each system is placed in a leaky cavity. Emission from a pair of such cavities, via a 50:50 beam splitter (BS), is detected in detectors D_+ or D_-, and conditionally leads to entangled qubit states.

which are monitored by two vacuum-discriminating detectors, D_+ and D_-, with efficiency η.

The EO scheme proceeds as follows. Firstly, both qubits are prepared in the state $|+\rangle = (|\uparrow\rangle + |\downarrow\rangle)/\sqrt{2}$. We then implement the following sequence of operations: (i) Apply an optical π pulse to each qubit, coherently pumping the population in the $|\downarrow\rangle$ state into the $|e\rangle$ state. (ii) Wait for up to a time t_{wait} for a photodetection event in either D_+ or D_-. (iii) Wait for a further time t_{relax} for any remaining excitation in the qubit-cavity systems to relax. (iv) Apply an X operation to both qubits, coherently flipping the spins as $|\uparrow\rangle \rightarrow |\downarrow\rangle$ and $|\downarrow\rangle \rightarrow |\uparrow\rangle$. (v) Repeat steps (i)–(iii).

Appropriate values for t_{wait} and t_{relax} are determined by the system parameters, as discussed below. If zero or two photodetection events are observed on either round of the procedure, the EO failed, and the qubits must be reprepared before reattempting the EO. On the other hand, if one (and only one) photodetection event is observed on each round of the protocol, the EO has succeeded, and a maximally entangled state is prepared *with unit fidelity*, even in the presence of photon loss. This *double-heralding* technique turns out to be exceedingly robust against the most common experimental errors.

We analyzed the scheme in detail using the quantum trajectories formalism [17]. For clarity, we first consider the ideal case, in which the detectors have unit efficiency ($\eta = 1$), and spontaneous emission of photons from the transition $|e\rangle \rightarrow |\downarrow\rangle$ into modes other than the cavity mode is neglected. During time periods where no detector clicks are observed, the conditional state of the system, in the interaction picture, evolves smoothly according to the effective Hamiltonian ($\hbar = 1$),

$$H_{\text{eff}} = \sum_{i=A,B} \frac{g_i}{2}(|\downarrow\rangle_{ii}\langle e|\hat{c}_i^\dagger + \text{H.c.}) - i \sum_{i=A,B} \kappa_i \hat{c}_i^\dagger \hat{c}_i.$$

Here, g_i denotes the Jaynes-Cummings coupling between the $|e\rangle_i \leftrightarrow |\downarrow\rangle_i$ transition and the mode of the ith cavity, and $\hat{c}_i$ is the corresponding annihilation operator. For the purpose of illustrating the ideal case, we assume that systems A and B are identical, such that $g_A = g_B = g$ and $\kappa_A = \kappa_B = \kappa$, and that $\kappa \geqslant g$.

When a single click is observed in detector $D_\pm$, the state of the whole system discontinuously evolves as $|\psi(t)\rangle \rightarrow \hat{c}_\pm |\psi(t)\rangle$, where $\hat{c}_\pm = (\hat{c}_A \pm \hat{c}_B)/\sqrt{2}$ denotes the corresponding jump operators. Thus, after steps (i) and (ii) of the entangling protocol, conditioned on observing a detector click at time $t_1 \leqslant t_{\text{wait}}$, the unnormalized state of the whole system is

$$|\tilde{\psi}(t_1)\rangle = \alpha(t_1)|\Psi_\pm\rangle + \alpha(t_1)\beta(t_1)\frac{|\downarrow,0;e,0\rangle \pm |e,0;\downarrow,0\rangle}{\sqrt{2}} + 2\alpha^2(t_1)\frac{|\downarrow,0;\downarrow,1\rangle \pm |\downarrow,1;\downarrow,0\rangle}{\sqrt{2}}. \quad (1)$$

Here, $|q_A, p_A; q_B, p_B\rangle$ is the state of the whole system, with $q_{A(B)}$ and $p_{A(B)}$ denoting the states of matter system A (B) and cavity mode A (B), respectively, $|\Psi^\pm\rangle = (|\downarrow,0;\uparrow,0\rangle \pm |\uparrow,0;\downarrow,0\rangle)/\sqrt{2}$ are maximally entangled states, $\alpha(t) = -ig/(4\sqrt{\kappa^2 - g^2})(e^{-\Gamma_{\text{slow}}t/2} - e^{-\Gamma_{\text{fast}}t/2})$ and $\beta(t) = \frac{1}{2}(1 + \kappa/\sqrt{\kappa^2 - g^2})e^{-\Gamma_{\text{slow}}t/2} + \frac{1}{2}(1 - \kappa/\sqrt{\kappa^2 - g^2})e^{-\Gamma_{\text{fast}}t/2}$, where $\Gamma_{\text{fast}} = \kappa + \sqrt{\kappa^2 - g^2}$ and $\Gamma_{\text{slow}} = \kappa - \sqrt{\kappa^2 - g^2}$. In order to obtain a detector click with high probability, we require $t_{\text{wait}} \gtrsim 3\Gamma_{\text{slow}}^{-1}$.

Equation (1) implies that it is possible to observe a *second* detector click on the *first* round of the protocol. However, realistic photodetectors typically cannot resolve two photons arriving in quick succession [18]. Within the quantum trajectories description, this can be simulated by assuming that no information is available from either detector after the first click. After a time $t_{\text{relax}} \gg \Gamma_{\text{slow}}^{-1}$, the system decoheres to the state $\rho = N^{-1}|\Psi_\pm\rangle\langle\Psi_\pm| + (1 - N^{-1})|\downarrow\downarrow\rangle\langle\downarrow\downarrow|$ where $N = 1 + |\beta(t_1)|^2 + |\alpha(t_1)|^2$. The undesirable second term in ρ is removed by applying steps (iv) and (v) of the entangling procedure. If a photodetection occurs on the second round, the final state of the system is a pure, maximally entangled state. If the two clicks are observed in the same (different) detector(s), the final state is $|\Psi^+\rangle$ ($|\Psi^-\rangle$). The four possible successful outcomes occur with probability $\frac{1}{8}$, leading to a total success probability of $p = \frac{1}{2}$.

We also analyzed the scheme in the nonideal case, allowing for imperfect detector efficiency $\eta < 1$, and finite spontaneous emission into free space ($\gamma_1 = \gamma_2 = \gamma > 0$). These imperfections do not reduce the fidelity of the final state, but do reduce the success probability [see Fig. 2(a)].

The dominating experimental imperfections that do reduce the fidelity are: (1) decoherence of the matter qubits, (2) dark counts in the detectors, and (3) imperfect mode matching of the photons incident on the beam splitter. Firstly, the effect of spin decoherence depends on the way the cluster states are generated, and can be estimated by comparing the spin decoherence time t_{d} with the "clock time" $t_{\text{c}} \sim 10\Gamma_{\text{slow}}^{-1}$ at which the EO can be repeated. If the preparation of cluster states is performed in parallel, the typical time overhead is m clock cycles (see below). Thus the average age of a qubit the moment it is added to the cluster is $(m/2)t_{\text{c}}$, and $m \lesssim 8$ for reasonable detector efficiencies. Assuming a reasonable cavity qubit coupling, $g = 100\gamma$, and critically damped cavities ($g \approx \kappa$), the size of errors due to spin decoherence is given by $\varepsilon \sim (m/2)t_{\text{c}}/t_{\text{d}} \sim 0.4\gamma^{-1}/t_{\text{d}}$. For instance, for the NV-diamond system ($\gamma^{-1} = 25$ ns [19] and $t_{\text{d}} = 32$ μs [20]), we have $\varepsilon \sim 3 \times 10^{-4}$.

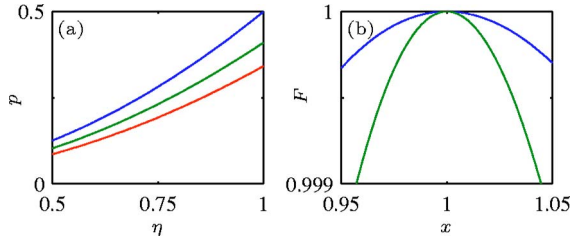

FIG. 2. (Color online) (a) Probability of success p vs the detector efficiency η after both rounds of the entangling procedure, plotted for different values of the spontaneous emission rate $\gamma = \{0, 0.1\Gamma_{\text{slow}}, 0.2\Gamma_{\text{slow}}\}$ (top to bottom). Other parameters are $g = 0.3$ and $\kappa = 1$. (b) Fidelity of the entangled qubit pair for imperfectly mode-matched photons. Upper curve: fidelity for nonidentical leakage rates, $x = \kappa_1/\kappa_2$, taking $g_1 = g_2$. Lower curve: fidelity for nonidentical coupling parameters, $x = g_1/g_2$, taking $g_2 = 0.3$ and $\kappa_1 = \kappa_2 = 1$.

Secondly, detector dark counts on either round of the EO can lead to a spurious "success" of the EO, which can reduce the fidelity of the entanglement. For existing avalanche-photodiode detectors, dark count rates are typically $\Gamma_{\text{dc}} < 500\ \text{s}^{-1}$ [21]. The effect on the cluster fidelity can be made negligible by observing the detector output only for the window $t_{\text{wait}} \sim 3\Gamma_{\text{slow}}^{-1}$ (~ 1 ns for NV diamond), leading to an error probability of $p_{\text{dc}} = \Gamma_{\text{dc}} t_{\text{wait}} \sim 10^{-7}$.

Finally, imperfect mode matching of the photons emitted by the matter qubit-cavity systems reduces the fidelity, because the photons carry information regarding their origin. Nonidentical central frequencies and spatiotemporal mode shapes of the photons can reduce the fidelity. The frequency of the photons emitted from cavity i depends on the frequencies of both the $|\downarrow\rangle_i \leftrightarrow |e\rangle_i$ transition ($\omega_{\downarrow e,i}$) and the cavity mode ($\omega_{\text{cav},i}$). The $\omega_{\downarrow e,i}$'s can be tuned independently, e.g., by using local electric and magnetic fields. The $\omega_{\text{cav},i}$'s can also be tuned, e.g., by using strain-tunable silica microcavities [22], or piezoelectrically tuned fiber-optic microcavities [23]. The spatiotemporal mode shapes of the emitted photons depend on the g_i's and κ_i's of the respective cavities, which are more difficult to calibrate once the cavities have been fabricated. However, the EO is rather robust to such mismatches [see Fig. 2(b)]: mismatches of a few percent reduce the fidelity by less than 10^{-3}.

The next step towards scalable quantum computers is linking qubits together into cluster states, using the EO described above. A cluster state of qubits $\{q_1, q_2, \ldots q_N\}$ can be represented graphically by a collection of qubit nodes connected by edges connecting neighboring qubits, as depicted in Fig. 3(a). A linear cluster of N qubits (a *chain*) may be represented in the form $|C\rangle_{1\ldots N} = (|\uparrow\rangle_1 + |\downarrow\rangle_1 Z_2)(|\uparrow\rangle_2 + |\downarrow\rangle_2 Z_3)\ldots(|\uparrow\rangle_N + |\downarrow\rangle_N)$, where Z_i represents the Pauli phase-flip operation acting on qubit i. Such linear clusters can be grown using our EO, as we now describe. Given a cluster $|C\rangle_{2\ldots N}$, qubit 1 can be added to the end of the cluster by first preparing qubit 1 in the state $|+\rangle_1 \equiv |\downarrow\rangle_1 + |\uparrow\rangle_1$ and then applying the EO to qubits 1 and 2. If the EO is successful, the resulting state is of the form $(|\uparrow\rangle_1|\downarrow\rangle_2 \pm |\downarrow\rangle_1|\uparrow\rangle_2 Z_3)|C\rangle_{3\ldots N}$, depending on whether both clicks were observed in the same detector. This can be transformed into a cluster state by applying the local operations $H_1 X_2$ or $X_1 H_1 X_2$, conditional on the outcome of the EO (here H_i is the Hadamard operation, and X_i the Pauli operator implementing a bit flip). If the EO fails, the state of qubit 2 is, in general, unknown. However, measuring qubit 2 in the computational basis removes qubit 2 from the cluster, but projects qubits $\{3, \ldots, N\}$ back into a pure cluster state. Therefore, failure of the EO causes the original cluster to shrink by one qubit.

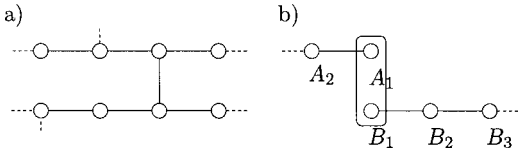

FIG. 3. Cluster states. (a) The qubits (circles) are entangled with their nearest horizontal neighbor via EOs (depicted by lines between the qubits), and gates between computational qubits are incorporated by the vertical lines. (b) Linear clusters can be joined together by applying the EO between qubits A_1 and B_1, and subsequently performing single-qubit operations and measurements.

Repeatedly applying this procedure allows long chains to be grown. However, the theoretical upper limit on the success probability of our EO is $p = \frac{1}{2}$, and therefore, with this procedure one cannot create large clusters efficiently. If recycling of the clusters after a failure [16] is not performed, the average number of EOs required to create a cluster of m qubits is $N_{\text{EO}} = \sum_{i=1}^{m-1} p^{-i}$.

A way around this problem is a "divide and conquer" approach, in which short chains are grown separately and then joined to a longer cluster using the EO together with local operations. The EO can be used to join two clusters, as shown in Fig. 3(b). These chains, A and B of length N and m, respectively, can be joined together by first performing the local operation X_{A_1}, then applying the EO between qubits A_1 and B_1, and measuring B_1 in the basis $|\pm\rangle_{B_1} \equiv |\downarrow\rangle_{B_1} \pm |\uparrow\rangle_{B_1}$. If the EO was successful, the remaining qubits are left in a state which may be transformed, via a local operation on qubit A_1, into a cluster state of length $N+m-1$, of qubits $\{A_N, \ldots, A_1, B_2, \ldots, B_m\}$. If the EO fails, qubit A_1 must be measured in the computational basis, and the original cluster state shrinks by one qubit. Thus the average length of the new cluster is $L = p(N+m-1) + (1-p)(N-1)$. In order that the cluster grows on average, we require $L > N$, which implies that length of the short chains should satisfy $m > 1/p$.

Chains of fixed length m can be grown independently using the EO, either by sequentially adding single qubits to the end of a cluster, or by joining subchains together. Growing these m-chain adds a constant overhead cost to the cluster generation process. For example, growing a 4-chain (without recycling) requires on average $p^{-3} + p^{-2} + p^{-1}$ applications of the EO, and each attempt to join such a chain adds on average $4p-1$ qubits to the large cluster, leading to a total cost of $C_4 = (p^{-3} + p^{-2} + p^{-1} + 1)/(4p-1)$ EOs per qubit added to the large cluster. A 5-chain can be grown by joining two 3-chains together, a 9-chain can be grown by joining two 5-chains, and so on. Joining such chains to a longer cluster leads to total costs of $C_5 = (2p^{-3} + 2p^{-2} + p^{-1} + 1)/(5p-1)$ and $C_9 = (4p^{-4} + 4p^{-3} + 2p^{-2} + p^{-1} + 1)/(9p-1)$ EOs per qubit, respec-

tively. For example, for $p \approx 0.24$ (or $\eta = 70\%$ with $\gamma = 0$), we require $m = 5$, and we find $C_5 = 775$. A modest improvement in detector efficiency dramatically reduces the overhead cost: for $\eta = 85\%$ and $\gamma = 0$, we find $C_4 = 73.4$. There may be more efficient schemes for growing linear clusters using our EO (e.g., employing recycling of small clusters [16]) which yield lower overhead costs.

In order to build linear chains into two-dimensional cluster states capable of simulating arbitrary logic networks, crosslinks between linear chains must be constructed [15]. Such a link can be created by first using the EO to create an *I*-shaped cluster [see Fig. 3(a)] offline, for some fixed cost. Provided the arms of this *I* cluster are sufficiently long, the EO can be used to join the *I* cluster to a pair of linear clusters with a high probability, and therefore create a crosslink between the clusters. This leads to a constant overhead cost per crosslink added to the cluster, and hence per two-qubit logic operation in the computation. Other methods for creating two-dimensional clusters, e.g., using microclusters [15] or redundant encoding [16], have also been proposed.

Our proposal has a number of very desirable features with respect to practical implementations. Firstly, our scheme requires only a simple level structure and single-qubit operations. Secondly, photon loss does not reduce the fidelity of the entangled states, but merely adds to the overhead cost. Thirdly, owing to the simplicity of the optical networks used, mode matching should be relatively straightforward. Fourthly, the scheme is inherently *distributed*, and our scheme lends itself naturally to distributed applications, such as quantum repeaters [24] and cryptography [25]. Finally, many of the techniques described here have been demonstrated experimentally, and the system requirements needed to create high-fidelity cluster states do not seem prohibitively restrictive.

Note added. While preparing this manuscript, we became aware of an alternative scheme that may also be used for generating cluster states of matter qubits [26].

We thank Tim Spiller and Bill Munro for valuable discussions. The authors are supported by the E.U. Nanomagiqc and Ramboq projects.

[1] J. I. Cirac and P. Zoller, Phys. Rev. Lett. **74**, 4091 (1995).
[2] F. Jelezko *et al.*, Phys. Rev. Lett. **92**, 076401 (2004).
[3] E. Pazy *et al.*, Europhys. Lett. **62**, 175 (2003).
[4] A. Nazir *et al.*, Phys. Rev. Lett. **93**, 1505021 (2004).
[5] M. Riebe *et al.*, Nature (London) **429**, 734 (2004).
[6] M. D. Barrett *et al.*, Nature (London) **429**, 737 (2004).
[7] C. Cabrillo *et al.*, Phys. Rev. A **59**, 1025 (1999); S. Bose *et al.*, Phys. Rev. Lett. **83**, 5158 (1999); X. L. Feng *et al.*, *ibid.* **90**, 217902 (2003); L.-M. Duan and H. J. Kimble, *ibid.* **90**, 253601 (2003); D. E. Browne, M. B. Plenio, and S. F. Huelga, *ibid.* **91**, 067901 (2003); C. Simon and W. T. M. Irvine, *ibid.* **91**, 110405 (2003).
[8] I. E. Protsenko *et al.*, Phys. Rev. A **66**, 062306 (2002).
[9] X. Zou and W. Mathis, e-print quant-ph/0401042.
[10] L.-M. Duan *et al.*, Quantum Inf. Comput. **4**, 165 (2004).
[11] J. M. Taylor *et al.*, e-print cond-mat/0407640.
[12] R. Raussendorf and H. J. Briegel, Phys. Rev. Lett. **86**, 5188 (2001).
[13] E. Knill, R. Laflamme, and G. J. Milburn, Nature (London) **409**, 26 (2001).
[14] N. Yoran and B. Reznik, Phys. Rev. Lett. **91**, 037903 (2003).
[15] M. A. Nielsen, Phys. Rev. Lett. **93**, 040503 (2004).
[16] D. E. Browne and T. Rudolph, e-print quant-ph/0405157.
[17] H. J. Carmichael, *An Open Systems Approach to Quantum Optics*, Lecture Notes in Physics, Vol. 18 (Springer, Berlin, 1993).
[18] P. Kok and S. L. Braunstein, Phys. Rev. A **61**, 042304 (2000).
[19] A. Beveratos *et al.*, Eur. Phys. J. D **18**, 191 (2002).
[20] T. A. Kennedy *et al.*, Phys. Status Solidi B **233**, 416 (2002).
[21] SPCM data sheet at http://optoelectronics.perkinelmer.com
[22] W. VonKlitzing *et al.*, New J. Phys. **3**, 14 (2001).
[23] Jason Smith (private communication).
[24] H. J. Briegel *et al.*, Phys. Rev. Lett. **81**, 5932 (1998).
[25] A. K. Ekert, Phys. Rev. Lett. **67**, 661 (1991).
[26] Y. L. Lim, A. Beige, and L. C. Kwek, e-print quant-ph/0408043.